Acta Crystallographica Section D
Biological Crystallography
ISSN 0907-4449

Direct experimental observation of the hydrogen-bonding network of a glycosidase along its reaction coordinate revealed by atomic resolution analyses of endoglucanase Cel5A

Annabelle Varrot and Gideon J. Davies*

Structural Biology Laboratory, Department of Chemistry, The University of York, Heslington, York YO10 5YW, England

Correspondence e-mail: davies@ysbl.york.ac.uk

Received 14 August 2002
Accepted 19 December 2002

PDB References: Cel5A Michaelis complex, 1h2j, r1h2jsf; Cel5A glycosyl-enzyme intermediate, 1h11, r1h11sf; Cel5A–product complex, 1hf6, r1hf6sf.

Non-covalent interactions between protein and ligand at the active centre of glycosidases play an enormous role in catalysis. Dissection of these hydrogen-bonding networks is not merely important for an understanding of enzymatic catalysis, but is also increasingly relevant for the design of transition-state mimics, whose tautomeric state, hydrogen-bonding interactions and protonation contribute to tight binding. Here, atomic resolution (∼1 Å) analysis of a series of complexes of the 34 kDa catalytic core domain of the *Bacillus agaradhaerens* endoglucanase Cel5A is presented. Cel5A is a 'retaining' endoglucanase which performs catalysis *via* the formation and subsequent breakdown of a covalent glycosyl-enzyme intermediate *via* oxocarbenium-ion-like transition states. Previous medium-resolution analyses of a series of enzymatic snapshots has revealed conformational changes in the substrate along the reaction coordinate (Davies *et al.*, 1998). Here, atomic resolution analyses of the series of complexes along the pathway are presented, including the 'Michaelis' complex of the unhydrolysed substrate, the covalent glycosyl-enzyme intermediate and the complex with the reaction product, cellotriose. These structures reveal intimate details of the protein–ligand interactions, including most of the carbohydrate-associated H atoms and the tautomeric state of crucial active-centre groups in the pH 5 orthorhombic crystal form and serve to illustrate the potential for atomic resolution analyses to inform strategies for enzyme inhibition.

1. Introduction

Catalysis by glycosidases involves the harnessing of many non-covalent interactions between enzyme and substrate. Individual hydrogen bonds may contribute in excess of 22 kJ mol^{-1} at the transition state (Namchuk & Withers, 1995). In order both to understand catalysis and to harness such interactions for the rational design of transition-state mimics, both as mechanistic probes and therapeutic agents, a complete description of the complex hydrogen-bonding networks is desired. Furthermore, the protonation and tautomeric state of putative transition-state mimics is of fundamental and rapidly evolving importance for glycosidase inhibition (see, for example, Notenboom *et al.*, 2000; Varrot *et al.*, 1999; Williams *et al.*, 2000) and experimental strategies to address these issues are a major growth area. Clearly, the unambiguous observation of the direction of hydrogen bonds and of protonation and tautomeric states in the active centre is possible with X-ray crystallography only when performed at 'atomic' resolution (Dauter *et al.*, 1997; Sheldrick & Schneider, 1997), but comparatively few systems are amenable to such analyses.

The endoglucanase Cel5A from *Bacillus agaradhaerens* (Davies, Sinnott *et al.*, 1998) is an ideal model for the study of a glycosidase active centre at atomic resolution. Cel5A is a multi-modular enzyme composed of a 303-amino-acid (34 kDa) catalytic core domain, two fibronectin type III domains and a carbohydrate-binding module (classified as a CBM family 5 moiety). The orthorhombic crystal form of the Cel5A catalytic core domain, grown at pH 5, diffracts to approximately 1 Å and both native and a putative transition-state mimic complex have previously been reported at atomic resolution (Davies, Mackenzie *et al.*, 1998; Varrot *et al.*, 1999).

Cel5A is a retaining glycosidase which hydrolyses the β-1,4-glycosidic linkages in cello-oligosaccharides *via* a classical Koshland double-displacement mechanism in which a covalent glycoside-enzyme intermediate is formed and subsequently hydrolysed *via* oxocarbenium-ion-like transition states (Davies, Mackenzie *et al.*, 1998) (Fig. 1). Glu139 acts as the Brønsted acid/base catalyst and Glu228 as the nucleophile. Trapping of the various states along the reaction coordinate through the application of 2-deoxy-2-fluoro oligosaccharides and pH control has previously been demonstrated at medium resolution (Davies, Mackenzie *et al.*, 1998). Here, atomic resolution analysis of a series of complexes including the Michaelis complex, the covalent glycosyl-enzyme intermediate and the reaction product complex reveals intimate details of the protein–ligand interactions, including most of the carbohydrate-associated H atoms and the tautomeric state of crucial active-centre groups.

2. Experimental

The catalytic core domain of Cel5A from *B. agaradhaerens* was purified and crystallized in its orthorhombic form (space group $P2_12_12_1$) using ammonium sulfate as precipitant at pH 4.5–5.0, as described previously (Davies, Dauter *et al.*, 1998). Michaelis (2,4-dinitrophenyl-2-deoxy-2-fluoro-β-D-cellobioside as ligand) and product (cellotriose) complexes were obtained by incubating individual crystals with a small quantity of powdered ligand under constant observation. The covalent intermediate was obtained by first incubating protein at pH 7.0 for 3 h in the presence of a stoichiometric quantity of 2,4-dinitrophenyl-2-deoxy-2-fluoro-β-D-cellotrioside prior to crystallization at pH 4.6–5.0, as above.

Prior to data collection, crystals were transferred for 1–3 s into a solution comprised of the growth/soaking conditions supplemented with 20%(*v*/*v*) glycerol as a cryoprotectant. Single crystals were mounted in rayon-fibre loops and placed in a boiling nitrogen stream at 100 K. X-ray diffraction data were collected from a single crystal for each complex in turn. Data to atomic resolution were collected for the Michaelis, covalent intermediate and product complexes on beamlines BW7B, BW7A and X31, respectively, at the EMBL Hamburg Outstation using MAR Research image-plate detectors. All

Table 1
Data and model quality statistics for the 'atomic resolution snapshots' of Cel5A.

Outer resolution shell statistics are given in parentheses.

	Michaelis complex of 2,4-dinitrophenyl-2-deoxy-2-fluoro-β-D-cellobioside	Covalent 2-deoxy-2-fluoro-cellotriosyl-enzyme intermediate	Product (cellotriose) complex
Diffraction data			
Beamline (EMBL Hamburg)	BW7B	BW7A	X31
Resolution of data (Å)	40.00–1.15 (1.19–1.15)	20.00–1.08 (1.12–1.08)	20.00–1.15 (1.19–1.15)
R_{merge}†	0.054 (0.360)	0.064 (0.282)	0.053 (0.307)
Completeness (%)	99.6 (99.7)	99.7 (99.2)	98.9 (93.0)
$I/\sigma(I)$	29.3 (4.3)	22.0 (5.0)	24.8 (3.9)
Multiplicity	4.4 (3.7)	4.3 (3.5)	4.3 (3.4)
Refinement			
Reflections used in refinement	98396	119386	98264
Reflection:parameter ratio‡	3.63	4.3	3.76
R_{cryst}	0.117	0.108	0.114
R_{free}	0.136	0.125	0.137
R.m.s.d. 1–2 bonds (Å)	0.016	0.017	0.022
R.m.s. angle deviation (Å)	1.75	1.9	2.05
R.m.s.d. main-chain *B*	0.645	0.055	0.6
R.m.s.d. side-chain *B*	1.534	1.33	1.4
Average ligand chain *B* (Å^2)	12.9/11.5	9.2	15.7
Average solvent *B* (Å^2)	26.3	24.1	24.7
No. of protein atoms	2450	2484	2504
No. of ligand atoms	35/22	34	32
No. of solvent atoms	378	510	466
No. Ramachandran 'outliers'§	1 (Leu103)	1 (Leu103)	1 (Leu103)
PDB code	1h2j	1h11	1hf6

† $R_{merge} = \sum_{hkl}\sum_i |I_{hkl} - (I_{hkl})|/\sum_{hkl}\sum_i (I_{hkl})$. ‡ Not treating geometric restraints as 'observations'. § Calculated with *PROCHECK* (Laskowski *et al.*, 1993).

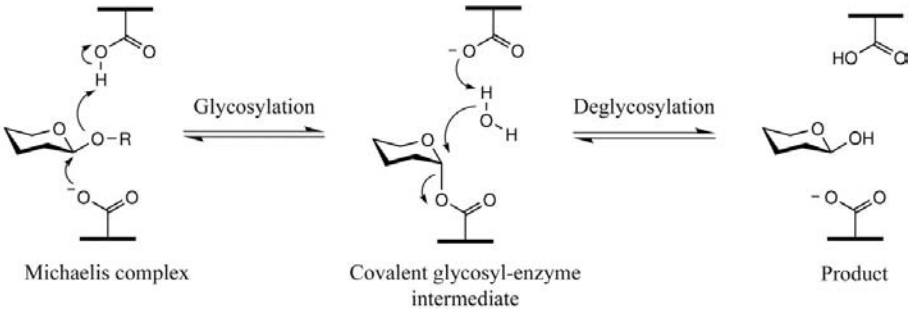

Figure 1
Schematic diagram of the enzymatic hydrolysis of β-glycosides by a retaining glycoside hydrolase. Net retention of anomeric configuration is achieved through the formation and subsequent breakdown of a covalent glycosyl-enzyme intermediate. Two enzymatic carboxylates act as nucleophile and acid/base, respectively. In the case of Cel5A these are Glu228 and Glu139, respectively.

data were processed and reduced using the *HKL* suite (Otwinowski & Minor, 1997) and all subsequent crystallographic computing used the *CCP*4 suite (Collaborative Computational Project, Number 4, 1994) unless otherwise stated.

Identical cross-validation (Brünger, 1992) reflections were used during refinement of all complex structures, having first been extended to the full resolution limit, and were used to monitor various refinement strategies such as the weighting of geometrical and temperature-factor restraints and the insertion of solvent water during maximum-likelihood refinement. Individual anisotropic refinement of the atomic displacement parameters was performed with *REFMAC* (Murshudov *et al.*, 1997, 1999) with 'riding' H atoms on the protein included. Manual corrections were performed with *QUANTA* (Accelerys, San Diego, CA, USA). Water molecules were initially introduced automatically using *REFMAC*/*ARP* (Lamzin & Wilson, 1993) from the *CCP*4 suite and were verified manually prior to coordinate deposition. Maximum-likelihood/σ_A (Read, 1986) weighted $mF_{\rm obs} - F_{\rm calc}$ difference maps were used to locate H-atom positions. Crystallographic data, including observed structure-factor amplitudes, have been deposited with the Protein Data Bank. Details of data and structure quality and PDB codes are given in Table 1.

3. Results

The 34 kDa catalytic domain of Cel5A catalytic presents a regular $(\alpha/\beta)_8$-barrel fold with a shallow-groove active site, accommodating five subsites, located at the C-terminal side of the barrel (Davies, Dauter *et al.*, 1998) (Fig. 2). As in the previous medium-resolution study (Davies, Mackenzie *et al.*, 1998), crystals of the Michaelis complex were obtained by harnessing a slowly turned-over 2-fluoro substrate at a low pH (4.6–5.0), where the enzyme displays greatly reduced activity owing to protonation of the catalytic nucleophile. Even under these conditions, 35% of the substrate is converted to the (trapped) glycosyl-enzyme intermediate (as has been observed with other Michaelis complex trapping; for example, Ducros *et al.*, 2002) and the Michaelis complex, of unhydrolysed 2,4-dinitrophenyl 2-deoxy-2-fluoro-β-D-cellobioside was observed with partial (~65%) occupancy. Structure and data-quality statistics are given in Table 1.

The unhydrolysed DNP-2-fluoro-2-deoxy-β-D-cellobioside shows clear distortion of the glucose ring in the -1 subsite from a chair to a $^1S_3$ skew-boat conformation, as observed both at intermediate resolution and also on other systems, notably the family 20 hexosaminidase (Tews *et al.*, 1996) and the family 7 endoglucanase Cel7B (Sulzenbacher *et al.*, 1996, 1997). Such distortion generates pseudo-axial orientation for the leaving group and presents the anomeric carbon to the nucleophile in an appropriate position, at a distance of 3.1 Å, for in-line attack, discussed further below. Unambiguous dissection of the tautomeric state of the catalytic nucleophile, Glu228, through unrestrained refinement of this residue yields OE2—CE and OE1—CE bond distances of 1.32 and 1.24 Å, consistent with a single bond from CE to OE2 (expected value 1.33 Å), reflecting the protonated state for OE2 at low pH, and a double bond between CE and OE1 (expected distance 1.22 Å). Given the approximate parameter-to-observation ratio of 3.63 (ignoring geometric restraints as observations), the *B* values of the relevant atoms (9.8, 9.7 and 12.1 Å^2 for CD, OE1 and OE2, respectively) and σ of 0.016 Å on the bond-length deviations (Table 1), the differences of 0.08 Å are at the 4σ level and would appear significant. Treatment of individual atom positional errors is clearly complex even in a maximum-likelihood-based refinement and, given much higher resolution data, inversion of the matrix following an unrestrained full-matrix refinement would be the most appropriate way to assess errors in individual positions. 15 of the 21 H atoms of the Michaelis complex are observed (13 at the 3σ level of the $F_o - F_c$ map and two at 2σ; data not shown), but those involved in the doubly occupied sugar in the -1 subsite, catalytically the most significant, are not observed in this complex.

Cel5A is a retaining glycosidase and consequently the second stable state along the reaction coordinate (Fig. 1) is the covalent glycosyl-enzyme intermediate. Accumulation of the subsequent covalent intermediate of Cel5A was achieved with 2,4-dinitrophenyl-2-fluoro-2-deoxy-β-D cellotrioside, reacted at pH 7.0 prior to crystallization. All sugar rings display $^4C_1$ chair conformation (Fig. 3). This complex, at 1.08 Å resolution, is a single species. Electron density reveals 21 of the 31 substrate H atoms unambiguously (visible at 2–3σ in the $F_o - F_c$ map), with a further eight displaying weaker (visible at 1–2σ) density (Fig. 4). Indeed, the only hydrogen not visible is that of the disordered hydroxymethyl group in the -1 subsite.

Almost complete dissection of the hydrogen bonding in the -1 to -3 subsites is possible and reveals features such as the doubly protonated His101 donating H atoms to both the O6 of

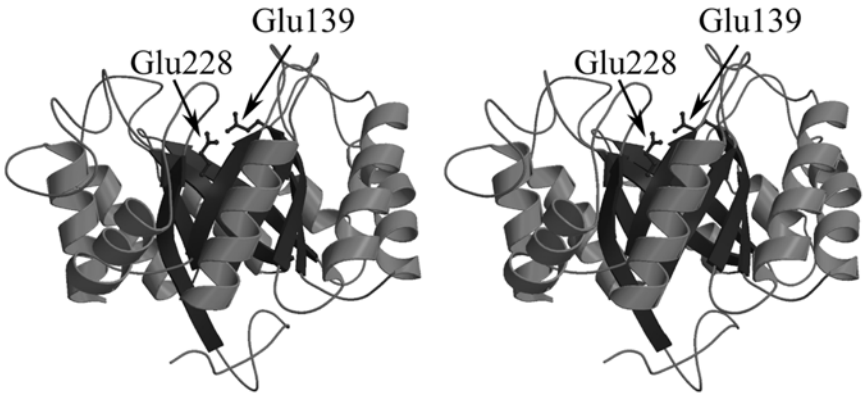

Figure 2
Three-dimensional structure of the 34 kDa catalytic core domain of Cel5A. The enzymatic carboxylates Glu139 (acid/base) and Glu228 (nucleophile) are shown in 'ball-and-stick' representation. The figure is shown in approximately the same orientation as in Fig. 5(*a*). This figure, in divergent (wall-eyed) stereo, was prepared with *BOBSCRIPT* (Esnouf, 1997).

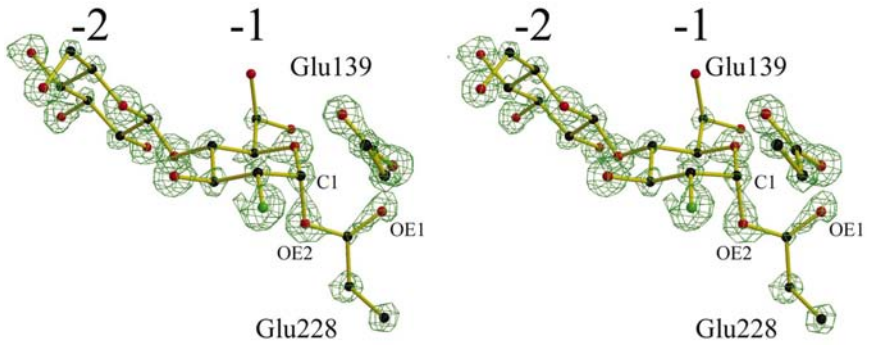

Figure 3
Electron density for the trapped 2-fluoro-2-deoxy-cellotriosyl-enzyme intermediate of Cel5A (only the −1 and −2 subsites are shown for clarity). The map is a maximum-likelihood-weighted $2F_{obs} - F_{calc}$ synthesis at 1.6 e Å^{-3} and is in divergent (wall-eyed) stereo.

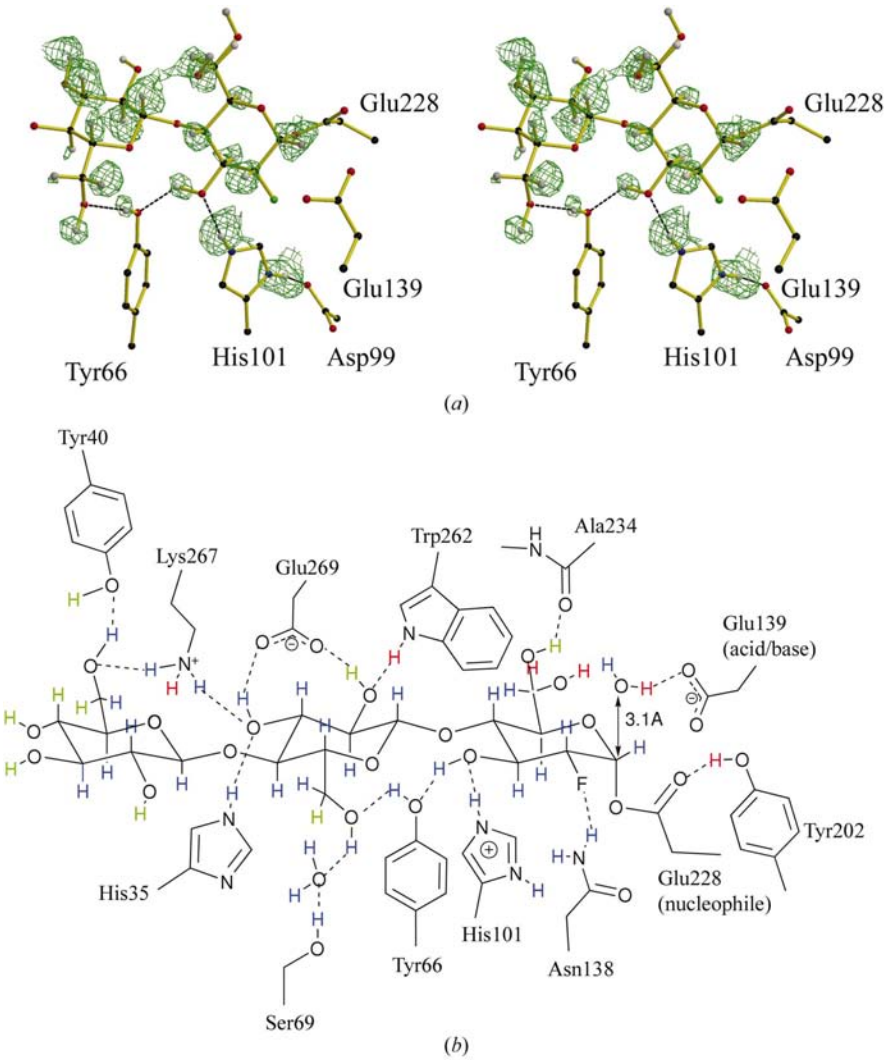

Figure 4
(*a*) Observed $F_{obs} - F_{calc}$ 'difference' electron density for the trapped covalent 2-fluoro-2-deoxy-cellotriosyl-enzyme intermediate of Cel5A. The map, contoured at +4σ, reveals the location of active-centre H atoms. Only density for the −1 and −2 subsites is shown for clarity. (*b*) Schematic figure of the hydrogen bonding within the Cel5A active centre. Experimentally determined H atoms are indicated in blue, those with weak density in green and those for which no electron density was observed in red.

the −1 subsite sugar and to Asp99. This unusual feature may simply reflect the low pH (5.0) of crystallization, approximately 2–3 pH units away from the pH optimum. Tyr66 forms a bridge between the 6-OH group of the −2 subsites to O3 of the −1 subsite, donating a hydrogen to O6 of the −2 subsite whilst acting as a hydrogen-bond acceptor from the 3-hydroxyl hydrogen of the −1 subsite sugar. A drawback of the 2-fluoroglucoside approach is that the interactions at the 2-position, which are known to be the most crucial for catalysis (Namchuk & Withers, 1995; Notenboom *et al.*, 1998), may not be dissected as this is both a fluoride substituent and the enzyme is trapped at low pH. The hydrogen bonding around this position cannot therefore be that of the active enzyme and dissection of the 2-OH interactions may require a complementary strategy (Notenboom *et al.*, 1998). The most likely difference with a natural ligand is that whilst Asn138 will still donate a hydrogen to the 2-OH group, as it does to 2-F observed here, the 2-hydroxyl hydrogen will probably be donated to the carbonyl O atom of the nucleophile (Notenboom *et al.*, 1998), requiring a reorientation of the side chain of the nucleophile, Glu228.

As with the medium-resolution work, the −1 subsite sugar in the cellotriose (product) complex is disordered (density not shown), reflecting both unfavourable binding and the potential for ring opening and mutarotation in this complex. Consequently, only eight of the possible 32 H atoms of the ligand are observed in this complex.

4. Discussion

Catalysis by glycosidases is driven, in no small measure, through the harnessing of non-covalent interactions both at the transition-state and elsewhere (Namchuk & Withers, 1995; Notenboom *et al.*, 1998). Atomic resolution analyses provide an experimental probe of such interactions and will, in future, allow dissection of tautomeric and protonation states of transition-state mimics: an emerging theme in glycosidase research (for example, Notenboom *et al.*, 2000; Varrot *et al.*, 1999; Williams *et al.*, 2000). Here, atomic resolution analysis confirms

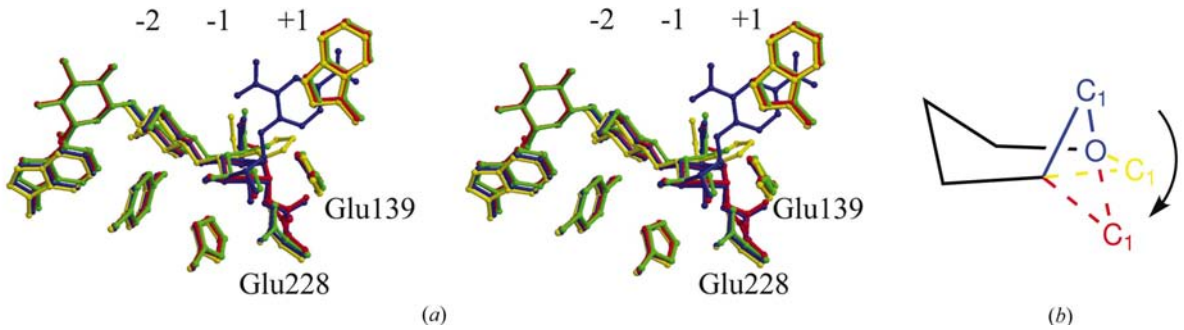

Figure 5
(*a*) Overlay of Cel5A structures along the reaction coordinate. Michaelis complex (plus the 35% of trapped intermediate) (blue), transition-state mimicking cellobio-imidazole (Varrot *et al.*, 1999) (yellow), covalent intermediate (red) and reaction product (green). A feature of these complexes is the static nature of the protein, with the exception of the nucleophile which rotates to avoid a steric clash with the 2-F substituent in the trapped 2-fluoro-glycosyl-enzyme intermediates. (*b*) Simplified schematic representation of the electrophilic migration of C1 along the reaction coordinate (with thanks to Dr David Vocadlo).

earlier proposals about substrate distortion (Davies, Mackenzie *et al.*, 1998; Sulzenbacher *et al.*, 1996; Tews *et al.*, 1996) and allow unparalleled description of the hydrogen-bonding network and protonation state of groups within the active centre, albeit in this case within the necessary constraints of a low-pH crystal form.

The first stable state along the reaction coordinate (Fig. 1) is the so-called 'Michaelis complex' of unhydrolysed substrate. Here, as previously, we observe a 'distorted' species in which the glucosyl moiety is twisted out of its relaxed $^4C_1$ (chair) conformation to a $^1S_3$ skew-boat with the leaving group now pseudo-axial. Thus far, experimental observation of such distortion has been limited to complexes in which a stable bulky leaving group in the +1 subsite 'locks' a non-hydrolysable substrate into the distorted conformation. One would expect, however, that microscopic reversibility demands that the attack of water on the trapped intermediate also occurs *via* similarly distorted species. For β-retaining enzymes working on *gluco*-configured substrates, $^1S_3$ skew-boat Michaelis complexes imply catalysis *via* the adjacent $^4H_3$ half-chair transition-state. That predictions made upon X-ray structure are fully consistent with the binding of transition-state mimics (Notenboom *et al.*, 2000; Varrot *et al.*, 1999) is good evidence for the potential of the structures of enzyme complexes in inhibitor design. Other classes of enzyme may perform catalysis *via* different potential transition-state conformations (Ducros *et al.*, 2002; Sabini *et al.*, 1999; Sidhu *et al.*, 1999; Varrot *et al.*, 2002; Zou *et al.*, 1999), which should eventually lead to the design of transition-state mimics which are specific for a given transition-state conformation as opposed to generic (Vasella *et al.*, 2002).

A number of glycosidase complexes have been reported in which ligands span the active centre and are not distorted (Hrmova *et al.*, 2001; Juers *et al.*, 2001; Lo Leggio *et al.*, 2000; Varrot *et al.*, 2001). We would contend that these binding modes do not demonstrate a 'limited requirement' for distortion: distortion from the $^4C_1$ chair to transition states maintaining C5, O5, C1 and C2 approximately coplanar and displaying pseudo-axial leaving groups is necessary for hydrolysis, fully consistent with stereoelectronic expectations, in-line nucleophilic attack and steric factors (Vasella *et al.*, 2002).

Although this distortion sounds complex, especially since it involves transitions (from $^1S_3 \rightarrow {}^4H_3 \rightarrow {}^4C_1$) between pyranoside rings whose nomenclature is difficult to follow, it is important to note that there is very little atomic movement along the reaction coordinate except the 'electrophilic migration' (Vocadlo *et al.*, 2001) of C1 towards the nucleophile (Fig. 5). Halfway between the Michaelis and intermediate conformations the anomeric carbon achieves coplanarity with C5, O5 and C2 and during catalysis this half-chair conformation is also sp^2 hybridized, generating the oxocarbenium-ion-like transition state (reflected in both kinetic isotope effect measurements and the tight binding of half-chair transition-state mimics (Davies *et al.*, 1997; Zechel & Withers, 1999, 2000). An overlay of the Michaelis, putative transition-state mimic (cellobiosyl-imidazole complex from Varrot *et al.*, 1999) and the covalent glycosyl-enzyme intermediate (Fig. 5) reveals very little atomic movement apart from this 'migration' of C1. Glycosidases of this class are very much 'lock-and-key' enzymes as described by Fischer (1894).

The conformational complexity exemplified by glycoside hydrolysis serves to illustrate that as protein crystallography enters the post-genomic 'high-throughput' era, atomic resolution analyses must represent a major goal if we are to define such features as hydrogen bonding, protonation and tautomeric states in order to both dissect mechanistic features and contribute appropriately to strategies for the design of powerful therapeutic agents. In cases where crystal quality or atomic mobility prevent unambiguous observation of hydrogen density using X-rays, neutron diffraction (for example, Helliwell, 1997) provides a powerful additional tool for hydrogen (deuterium) location at more modest resolutions.

The authors would like to acknowledge the enormous contribution of the late Martin Schülein (Novozymes A/S) to the glycosidase research in York. This work was supported by the Biotechnology and Biological Sciences Research Council

(BBSRC) and the European Union. GJD is a Royal Society University Research Fellow.

References

Brünger, A. T. (1992). *Nature (London)*, **355**, 472–475.

Collaborative Computational Project, Number 4 (1994). *Acta Cryst.* D**50**, 760–763.

Dauter, Z., Lamzin, V. S. & Wilson, K. S. (1997). *Curr. Opin. Struct. Biol.* **7**, 681–688.

Davies, G. J., Dauter, M., Brzozowski, A. M., Bjornvad, M. E., Anderson, K. V. & Schülein, M. (1998). *Biochemistry*, **37**, 1926–1932.

Davies, G. J., Mackenzie, L., Varrot, A., Dauter, M., Brzozowski, A. M., Schülein, M. & Withers, S. G. (1998). *Biochemistry*, **37**, 11707–11713.

Davies, G., Sinnott, M. L. & Withers, S. G. (1997). *Comprehensive Biological Catalysis*, Vol. 1, edited by M. L. Sinnott, pp. 119–209. London: Academic Press.

Ducros, V., Zechel, D. L., Murshudov, G. N., Gilbert, H. J., Szabo, L., Stoll, D., Withers, S. G. & Davies, G. J. (2002). *Angew. Chem. Int. Ed.* **41**, 2824–2827.

Esnouf, R. M. (1997). *J. Mol. Graph.* **15**, 133–138.

Fischer, E. (1894). *Ber. Dtsch. Chem. Ges.* **27**, 2985–2993.

Helliwell, J. R. (1997). *Nature Struct. Biol.* **4**, 874–876.

Hrmova, M., Varghese, J. N., De Gori, R., Smith, B. J., Driguez, H. & Fincher, G. B. (2001). *Structure*, **9**, 1005–1016.

Juers, D. H., Heightman, T. D., Vasella, A., McCarter, J. D., Mackenzie, L., Withers, S. G. & Matthews, B. W. (2001). *Biochemistry*, **40**, 14781–14794.

Lamzin, V. S. & Wilson, K. S. (1993). *Acta Cryst.* D**49**, 129–147.

Laskowski, R. A., McArthur, M. W., Moss, D. M. & Thornton, J. M. (1993). *J. Appl. Cryst.* **26**, 283–291.

Lo Leggio, L., Jenkins, J., Harris, G. W. & Pickersgill, R. W. (2000). *Proteins Struct. Funct. Genet.* **41**, 362–373.

Murshudov, G. N., Vagin, A. A. & Dodson, E. J. (1997). *Acta Cryst.* D**53**, 240–255.

Murshudov, G. N., Vagin, A. A., Lebedev, A., Wilson, K. S. & Dodson, E. J. (1999). *Acta Cryst.* D**55**, 247–255.

Namchuk, M. N. & Withers, S. G. (1995). *Biochemistry*, **34**, 16194–16202.

Notenboom, V., Birsan, C., Nitz, M., Rose, D. R., Warren, R. A. J. & Withers, S. G. (1998). *Nature Struct. Biol.* **5**, 812–818.

Notenboom, V., Williams, S. J., Hoos, R., Withers, S. G. & Rose, D. R. (2000). *Biochemistry*, **39**, 11553–11563.

Otwinowski, Z. & Minor, W. (1997). *Methods Enzymol.* **276**, 307–326.

Read, R. J. (1986). *Acta Cryst.* A**42**, 140–149.

Sabini, E., Sulzenbacher, G., Dauter, M., Dauter, Z., Jørgensen, P. L., Schülein, M., Dupont, C., Davies, G. J. & Wilson, K. S. (1999). *Chem. Biol.* **6**, 483–492.

Sheldrick, G. M. & Schneider, T. R. (1997). *Methods Enzymol.* **277**, 319–343.

Sidhu, G., Withers, S. G., Nguyen, N. T., McIntosh, L. P., Ziser, L. & Brayer, G. D. (1999). *Biochemistry*, **38**, 5346–5354.

Sulzenbacher, G., Driguez, H., Henrissat, B., Schülein, M. & Davies, G. J. (1996). *Biochemistry*, **35**, 15280–15287.

Sulzenbacher, G., Schülein, M. & Davies, G. J. (1997). *Biochemistry*, **36**, 5902–5911.

Tews, I., Perrakis, A., Oppenheim, A., Dauter, Z., Wilson, K. S. & Vorgias, C. E. (1996). *Nature Struct. Biol.* **3**, 638–648.

Varrot, A., Frandsen, T., Driguez, H. & Davies, G. J. (2002). *Acta Cryst.* D**58**, 2201–2204.

Varrot, A., Schülein, M., Fruchard, S., Driguez, H. & Davies, G. J. (2001). *Acta Cryst.* D**57**, 1739–1742.

Varrot, A., Schülein, M., Pipelier, M., Vasella, A. & Davies, G. J. (1999). *J. Am. Chem. Soc.* **121**, 2621–2622.

Vasella, A., Davies, G. & Böhm, M. (2002). *Curr. Opin. Chem. Biol.* **6**, 619–629.

Vocadlo, D. J., Davies, G. J., Laine, R. & Withers, S. G. (2001). *Nature (London)*, **412**, 835–838.

Williams, S. J., Notenboom, V., Wicki, J., Rose, D. R. & Withers, S. G. (2000). *J. Am. Chem. Soc.* **122**, 4229–4230.

Zechel, D. & Withers, S. G. (1999). *Comprehensive Natural Products Chemistry*, Volume 5, edited by D. Barton, K. Nakanishi & C. D. Poulter, pp. 279–314. Amsterdam: Elsevier.

Zechel, D. L. & Withers, S. G. (2000). *Acc. Chem. Res.* **33**, 11–18.

Zou, J.-Y., Kleywegt, G. J., Ståhlberg, J., Driguez, H., Nerinckx, W., Claeyssens, M., Koivula, A., Teeri, T. T. & Jones, T. A. (1999). *Structure*, **7**, 1035–1045.